JOURNAL OF THERMOPHYSICS AND HEAT TRANSFER
Vol. 23, No. 1, January–March 2009

Heat Transfer Enhancement in a Gas-Cooled Condenser Using Carbon Foams

W. Wu, J. Du, Y. R. Lin, J. Kapat, and L. C. Chow*
University of Central Florida, Orlando, Florida 32816
and
W. Notardonato
NASA Kennedy Space Center, Kennedy Space Center, Florida 32899

DOI: 10.2514/1.39078

Significant heat transfer enhancement by using carbon foam in the cold head of a cryocooler for liquefaction of cryogens is demonstrated. The development of an effective, lightweight and compact cold head for liquefaction of gaseous hydrogen and its subsequent densification to subcooled liquid hydrogen will require a condenser with high heat transfer coefficient and low pressure drop on the gas side. High-thermal-conductivity carbon foam is used to enhance the heat transfer coefficient. For convenience, as a first effort, this work uses air and vapor/liquid FC-87 to simulate helium and gaseous/liquid hydrogen, respectively. Experiments are conducted on carbon block foam and an alternative flow configuration called "corrugated" carbon foam, which has a lower flow resistance. Results of these experiments show that, compared with block carbon foam, corrugated carbon foam has a much lower pressure drop and a significant improvement in heat transfer performance. Experimental results of air and vapor/liquid FC-87 show that carbon-foam-based heat sinks can be 18 times better than conventional air-channel heat sinks at low speed (1 m/s).

Nomenclature

A_b	=	base area of heat transfer, m^2
c_p	=	heat capacity of the air, $J/kg \cdot K$
G_L	=	condensate FC-87 dripping rate, ml/ min
h_{air}	=	heat transfer coefficient of the air side, $W/m^2 \cdot K$
h_{fg}	=	latent heat of the FC-87, kJ/kg
h_{fc}	=	heat transfer coefficient of the FC-87 side, $W/m^2 \cdot K$
k	=	material thermal conductivity, $W/m \cdot K$
$\dot{m}_{air}$	=	air mass flow rate, kg/s
$\dot{m}_{fc}$	=	condensation mass flow rate, kg/s
Q_{air}	=	air cooling rate in the condenser, W
Q_{fc}	=	heat removal rate from FC-87 in the condenser, W
$T_{c,i}$	=	condenser air inlet temperature, K
$T_{c,o}$	=	condenser air outlet temperature, K
T_s	=	saturation temperature, K
T_w	=	temperature of wall separating air and FC-87, K
V	=	airflow speed, m/s
ΔT_m	=	log mean temperature difference, K
ρ_L	=	density of liquid FC-87, kg/m^3

I. Introduction

STORAGE of cryogens such as oxygen, methane, and hydrogen is essential for long-duration spaceflight missions. High-capacity mechanical cryocoolers for cryogenic storage are needed to reduce boil-off and provide pressure control for the cryogens, which makes it important to develop a highly effective, lightweight, and compact cold head for use in cryocoolers for cryogen storage applications through liquefaction and densification [1]. This ongoing effort is aimed at the optimal design, fabrication, and testing of a cold-head condenser for an ultracompact reverse-Brayton helium cryocooler that is based on the requirements of a liquid-hydrogen-fuel transportation and storage system, especially a liquid-hydrogen (LH_2) storage system on the moon and Martian surfaces [1,2].

The development of an effective cold head for liquefaction of gaseous hydrogen and its subsequent densification to subcooled liquid hydrogen will require a condenser with a high heat transfer coefficient on the cold-helium-gas side. The cold head is essentially a gas-cooled (helium-cooled) condenser. Because the dominant thermal resistance is on the cold-helium-gas side, miniaturization of the cold head requires a significant enhancement in heat transfer without creating an unacceptably high pressure drop on the cold-gas side. There are some relatively mature technologies for gas-side heat transfer enhancement that include an extended surface and a louvered fin surface with dimples or strips on the fins to improve the overall heat transfer coefficient [3]. Several researchers (for example, Calmidi and Mahajan [4] and Leong and Jin [5]) proposed to use open-cell aluminum foams to replace fin structures to reduce the size and weight of the heat transfer equipment. Even though metal foams possess a large specific surface area for heat transfer per unit volume, heat transfer enhancement is limited because of their low effective thermal conductivity due to high porosity. A good design for heat transfer enhancement incorporates carbon foam, which yields an optimal combination of convection and solid conduction.

Figure 1 shows a comparison in structure between aluminum foam and carbon foam [6]. Table 1 lists some typical properties of carbon foam and aluminum foam [5].† In comparison with aluminum foam, carbon foam has a smaller pore size and a larger surface area per unit volume. Carbon foam has thick ligaments and high thermal conductivity. The high thermal conductivity of carbon foam with the open interconnected cellular structure provides a potential for effective heat transfer enhancement.

Carbon foam has high thermal conductivity (100–230 $W/m \cdot K$ in plane and 50–80 $W/m \cdot K$ out of plane) because high-performance carbon fiber has an estimated thermal conductivity of greater than 1500 $W/m \cdot K$. The open-cell structure of the foam (see footnote †) gives it a large surface-area-to-volume ratio (greater than 40,000 m^2/m^3). There is a limited amount of information on heat transfer and pressure loss for gases in carbon foams. Gallego and Klett [6] and Klett et al. [7] reported the performance tests for air

Received 12 June 2008; revision received 11 August 2008; accepted for publication 14 August 2008.

*Department of Mechanical, Materials and Aerospace Engineering; lchow@mail.ucf.edu (Corresponding Author).

†Data available online at http://www.poco.com [retrieved Oct. 2008].

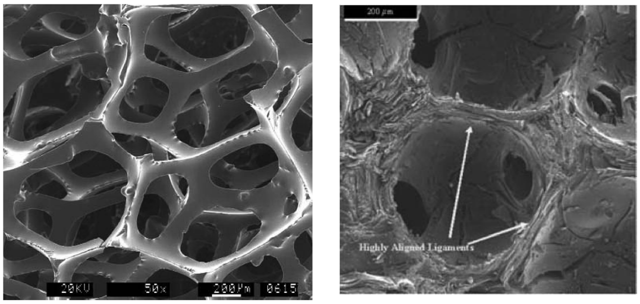

Fig. 1 A comparison in structure between aluminum foam (left) and carbon foam (right) [6].

passing through carbon foams and aluminum foams with several different configurations with frontal velocities from 1.5 to 4.3 m/s. Their study showed that carbon foam in the bulk (solid) form has a high heat transfer coefficient ($\sim$2600 $\mathrm{W/m^2 \cdot K}$) in comparison with aluminum foam ($\sim$250 $\mathrm{W/m^2 \cdot K}$). The pressure drop for the solid carbon foam is fairly high compared with that of aluminum foam. They found that the pressure drop for solid carbon foam could be significantly reduced by modifying the geometry of the foam, while keeping the heat transfer coefficient considerably higher than that of the aluminum foam. Gallego and Klett [6] measured the heat transfer coefficient and pressure drop for carbon foams with finned, pin-finned, blind holes (pin fin negative), and corrugated geometries. They found that with the corrugated and blind-hole carbon foams, the heat transfer coefficient increases, whereas the pressure drop decreases, compared with the solid carbon foam. Little work has been reported in the literature for an air-cooled condenser using carbon foam.

The motivation of this study is related to liquefaction of hydrogen using gaseous helium in a cryocooler. In the cold head, hydrogen gas is condensed through heat removal by cold helium with a small temperature difference. The dominant thermal resistance to heat removal is on the cold-gas side. Our primary objective is to explore the possibility of using carbon foam to significantly increase the heat transfer coefficient on the gas side in the cold head. We chose room air as the cold gas in our experiments for convenience. We simulated the small temperature difference by using FC-87 as the condensing fluid. FC-87 has a saturated temperature of 30°C at 1 atm. We noted the difference between this study and hydrogen liquefaction. Further tests will need to be conducted with the actual fluids under realistic application conditions in the future.

Condensation rates of FC-87 were measured for airflow speeds in the range of 0.17 to 1.0 m/s. Performance tests were conducted for three different cases: no carbon foam, solid carbon foam, and corrugated carbon foam. The effects of carbon foam and its configuration on heat transfer and pressure drop were investigated.

Table 1 Properties of carbon foam and aluminum foam [5][a]

Property	Al foams	Carbon foams
Ligament thickness, μm	100–420	$\sim$500
Pore size, mm	1–2	0.350
Porosity	>0.9	0.7–0.8
Effective k, $\mathrm{W/m \cdot K}$	5–9	100–230
Specific area, $\mathrm{m^2/m^3}$	800–2800	$>40,000$

[a]Data available online at http://www.poco.com.

II. Experimental Setup for an Air-Cooled FC-87 Condenser

Figure 2 is a diagram of the experimental setup for air-cooled FC-87 condensation. It consists of a container with saturated FC-87. A heater is immersed in the FC-87 liquid at the bottom for FC-87 vapor generation and control of temperature and pressure inside the container. Air flows through a 5 by 1 cm rectangular channel. The channel is 5 cm long. The channel is made of 1-cm-thick Plexiglas on three sides. On the fourth side, the wall is made of a 1.2-mm-thick copper plate. Figure 3a is a picture of the experiment and Fig. 3b shows the structure of the channel. Cold air passed through the channel, providing the heat removal required to condense the FC-87 vapor on the copper plate. Condensation on the Plexiglas walls was negligibly small when compared with the condensation on the copper surface because of the low thermal conductivity of Plexiglas. The FC-87 vapor condensed on the copper wall was collected through a cylindrical funnel below the condenser. The condensation rate was measured with a calibrated cylinder and a stop watch. The saturation temperature in the container was controlled at 30°C at a constant pressure of 1 atm by adjusting the power supply to the heater immersed in the FC-97 liquid using an automatic proportional–integral–derivative temperature controller [8]. Only the FC-87 collected on the condenser was measured. Any FC-87 that condensed on the inside wall of the container simply dripped back into the FC-87 liquid reservoir.

Carbon foam was placed in the rectangular channel for the purpose of enhancing heat transfer on the air side. The dimensions of the carbon foam are $5 \times 5 \times 1$ cm. The foam was attached to the copper plate with a silver-loaded epoxy (Pyro-Duct from Aremco). This epoxy ($\sim$250-μm-thick) has a thermal conductivity of 9 $\mathrm{W/m \cdot K}$, which gives an approximate value of 0.23×10^{-4} $\mathrm{m^2 \cdot K/W}$ for the

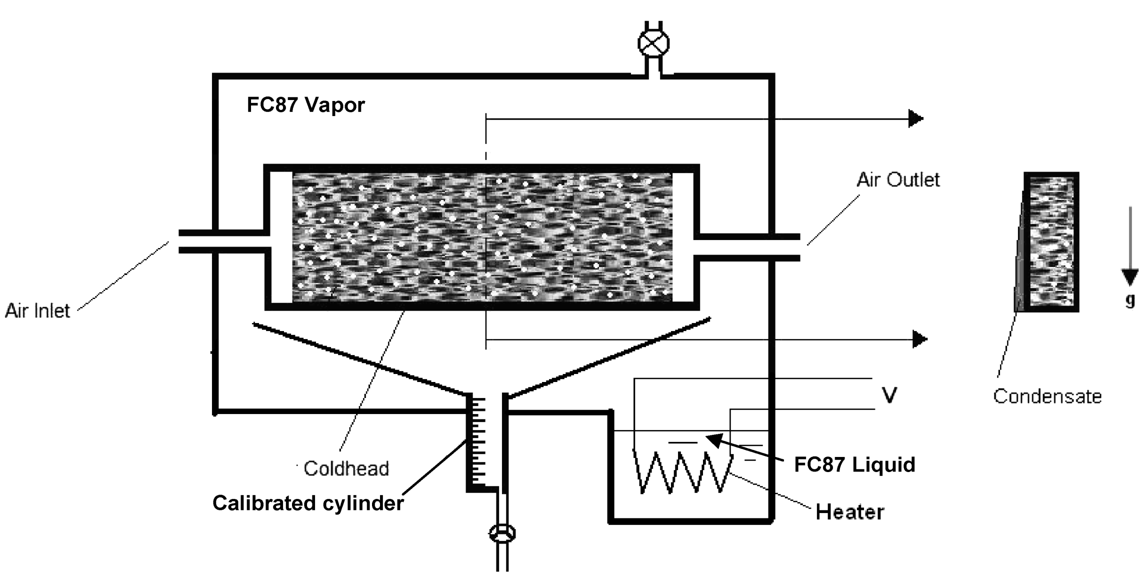

Fig. 2 Sketch of an air-cooled condenser in FC-87 vapor.

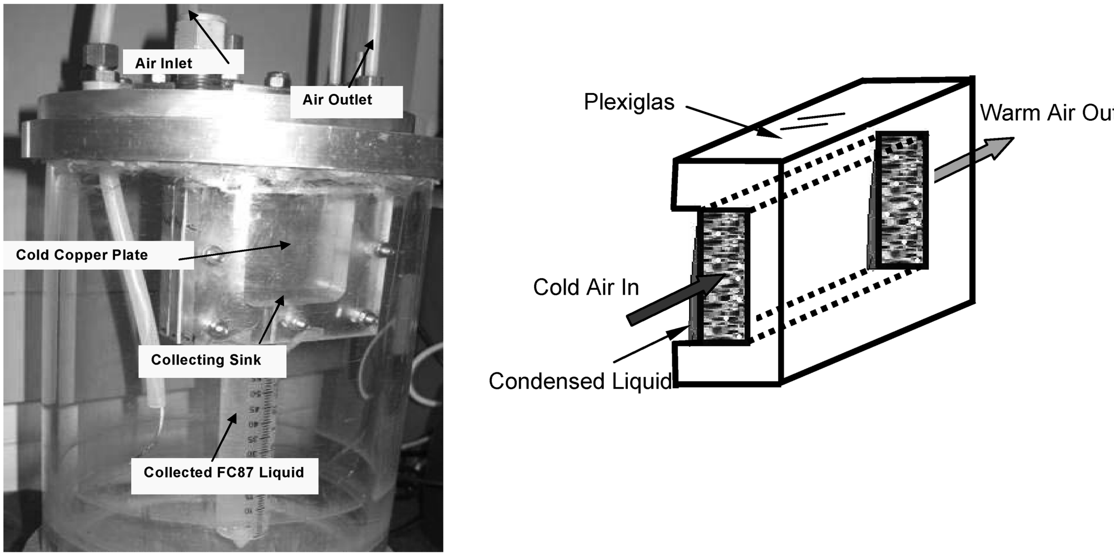

a) b)

Fig. 3 Setup of the condenser and the sketch of airflow channel with foam.

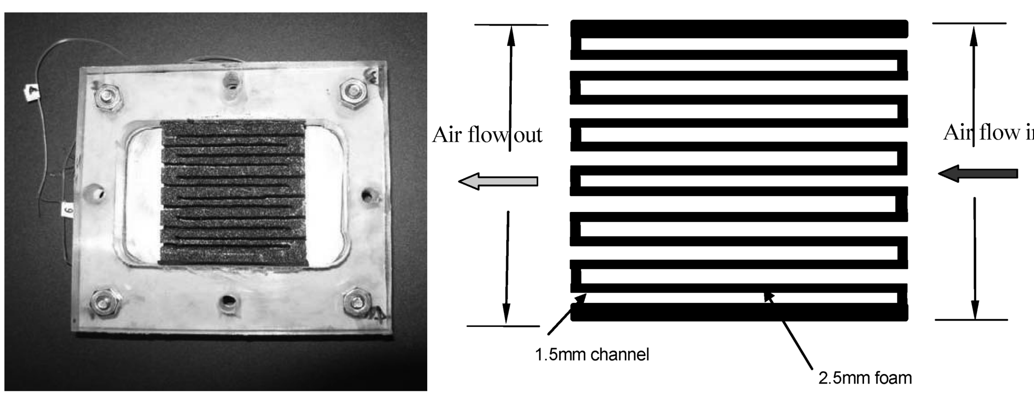

a) b)

Fig. 4 Corrugated foam.

thermal contact resistance between the foam and the copper plate.[‡] At the heat fluxes considered in our experiments, there is essentially no temperature drop (less than 0.05°C) across the epoxy layer. The foam occupies the entire cross section of the channel in the experiments.

Both solid and corrugated Poco foams [6] were used in our experiments. Figure 4 shows the picture of the corrugated foam and its dimensions.

III. Calculations of the Heat Transfer Coefficients of Air and FC-87

The variables measured in this experiment are the airflow rate, pressure drop across the air channel, inlet and outlet air temperatures, copper-plate temperatures, saturation temperature and pressure of FC-87, and condensation rate. The airflow rate was measured with a flow meter. The pressure difference across the foam samples was measured by pressure differential gauges. The air temperatures at the inlet and outlet were measured using 0.6 mm type-E thermocouples. The copper-plate surface temperature was measured by three thermocouples. One thermocouple was used to measure the saturation temperature in the container. All data collection was automated using a Keithley 2700 data acquisition/switching system interfaced to a computer. The pressure in the container was measured by a high-precision pressure gauge. The measured saturation temperature compared well with the saturation temperature of FC-87, based on the measured pressure of the FC-87. The condensation rate was measured by the volume of FC-87 collected in the calibrated cylinder.

The heat removed by the airflow is given by

$$Q_{\mathrm{air}} = \dot{m}_{\mathrm{air}} c_p (T_{c,o} - T_{c,i}) \tag{1}$$

The heat transfer coefficient on the air side is defined as

$$h_{\mathrm{air}} = \frac{Q_{\mathrm{air}}}{A_b \Delta T_m} \tag{2}$$

where ΔT_m is the log mean temperature difference and is given by

$$\Delta T_m = \frac{(T_w - T_{c,i}) - (T_w - T_{c,o})}{\ln[(T_w - T_{c,i})/(T_w - T_{c,o})]} \tag{3}$$

The amount of heat delivered during condensation of FC-87 is calculated by

$$Q_{fc} = h_{fg} G_L \rho_L \tag{4}$$

The heat transfer coefficient of the FC-87 side is determined by

[‡]Data available online at http://www.aremco.com [retrieved Oct. 2008].

Table 2 Properties of FC-87

Properties, 30°C	FC-87
T_s, °C	30
ρ_L, kg/m^3	1650
h_{fg}, kJ/kg	103

$$h_{fc} = \frac{Q_{fc}}{A_b(T_s - T_w)} \tag{5}$$

The properties of FC-87 at 1 atm are listed in Table 2.[§]

The airflow rate was measured by a flow meter that was calibrated with a high-precision mass flow meter, and the error was $\pm 1.2\%$. The error in temperature measurement was within $\pm 0.1°\mathrm{C}$ after we calibrated the Omega type-E thermocouples. The pressure drop across the foam samples was measured by differential pressure gauges, and the error was estimated to be 1% of the measured value. The uncertainty for pressure drop measurements was estimated to be less than ± 1 kPa and ± 50 Pa when measuring the solid and corrugated foams, respectively. The uncertainty of condensate volume measurement was ± 0.5 cm^3, with the minimum scale of 1 cm^3. The amount of condensate collected was at least 35 cm^3 for every experiment. The percentage error for condensation rate is less than 1.4%. For the case of solid carbon foam at the lowest-air-speed case, the estimated uncertainties in h_{air} and h_{fc} were determined to be 5 and 25%, respectively.

IV. Results and Discussion

Table 3 shows the heat transfer results for the empty channel without carbon foam. The average difference (error) between the air cooling rate Q_{air} and the FC-87 heating rate Q_{fc} is less than 10%. Thus, there is good agreement between the heat removed by the airflow and the heat provided by the FC-87 vapor via condensation. These results show that the air-side heat transfer coefficient is 25.9 W/m$^2\cdot$K at an air velocity of 1 m/s. Even at $V = 1$ m/s, the pressure drop across the empty air channel is negligible.

Table 4 shows the heat transfer results for the channel with the solid carbon foam. The heat transfer coefficient at $V = 1$ m/s is 341 W/m$^2\cdot$K, compared with 25.9 W/m$^2\cdot$K for an empty air channel. It should be noted that the condensation heat transfer coefficient of FC-87 varies between 806 and 1050 W/m$^2\cdot$K. So even with the carbon foam, the dominant thermal resistance is still on the air side.

Table 5 shows the air-side heat transfer results for corrugated carbon foam. The heat transfer coefficient of air with the corrugated carbon foam is 469 W/m$^2\cdot$K at $V = 1$ m/s, which is higher than that of solid carbon foam at 341 W/m$^2\cdot$K. The heat transfer performance of the corrugated carbon foam was moderately better than that of the solid foam. This trend in which the corrugated foam yields a better heat transfer coefficient than the solid foam agrees with results reported in [6]. The condensation heat transfer coefficients are comparable with those obtained in the experiments when solid foams were used.

Figure 5a shows the variation of air-side heat transfer coefficient with air velocity, and Fig. 5b shows the pressure drop versus air velocity for the empty channel, solid foam, and corrugated flow channels. Though there is less carbon material in the corrugated foam compared with the solid foam, corrugation changes the distribution of cold gas into the foam, which results in better heat transfer and lower pressure drop. Corrugating the carbon foam reduces the thermal path from the copper surface to the cold air, leading to smaller overall thermal resistance. Corrugation also increases the effective frontal length that the cold air enters into the foam structure. This decreases the air speed normal to the foam. The end result is more effective heat transfer enhancement through the carbon foam.

Table 3 Empty channel data

Air V, m/s	$T_{c,o}$, °C	$T_{c,i}$, °C	T_w, °C	T_s, °C	FC-87 G_L, ml/min	h_{air}, W/m$^2\cdot$K	Q_{air}, W	Q_{fc}, W	Error, %
0.17	21.2	20.6	29.5	29.5	0.020	12.7	0.059	0.057	4.1
0.25	21.0	20.5	30.0	30.1	0.023	14.6	0.068	0.065	4.4
0.34	20.5	20.1	29.9	30.0	0.025	16.7	0.079	0.071	11.4
0.50	21.0	20.7	30.1	30.2	0.032	21.2	0.101	0.091	11.8
0.76	21.0	20.8	29.8	29.9	0.038	24.1	0.115	0.108	7.2
1.0	20.8	20.6	29.6	29.7	0.040	25.9	0.128	0.113	13.1

Table 4 Solid carbon foam data

Air V, m/s	$T_{c,o}$, °C	$T_{c,i}$, °C	T_w, °C	T_s, °C	FC-87 G_L, ml/ min	h_{air}, W/m$^2\cdot$K	Q_{air}, W	Q_{fc}, W	Error, %	h_{fc}, W/m$^2\cdot$K
0.17	24.7	14.7	28.7	29.1	0.40	86.8	0.98	1.08	8.9	1050
0.25	24.5	11.3	29.6	30.4	0.70	103	1.95	1.98	1.6	1030
0.34	24.2	11.1	28.8	29.8	0.95	142	2.58	2.69	4.1	1040
0.50	17.7	8.7	28.7	30.1	1.00	198	2.65	2.83	6.4	828
0.76	16.6	7.7	27.8	29.9	1.50	281	3.96	4.25	6.9	819
1.0	15.5	7.6	27.4	29.8	1.75	341	4.65	4.96	6.1	806

Table 5 Corrugated carbon foam data

Air V, m/s	$T_{c,o}$, °C	$T_{c,i}$, °C	T_w, °C	T_s, °C	FC-87 G_L, ml/ min	h_{air}, W/m$^2\cdot$K	Q_{air}, W	Q_{fc}, W	Error, %	h_{fc}, W/m$^2\cdot$K
0.17	25.6	17.4	30.0	30.3	0.25	92.6	0.81	0.72	12.6	1030
0.25	27.3	14.4	29.8	30.4	0.65	125	1.90	1.84	3.3	1150
0.34	27.9	16.3	30.1	30.9	0.90	182	2.30	2.55	10.0	1200
0.50	24.2	11.5	28.4	30.1	1.50	279	3.77	4.25	11.4	971
0.76	19.8	10.1	28.5	30.7	1.60	380	4.30	4.53	5.1	832
1.0	18.1	6.1	26.6	30.4	2.80	469	7.07	7.93	10.8	822

[§]Data available online at http://www.3M.com [retrieved Oct. 2008].

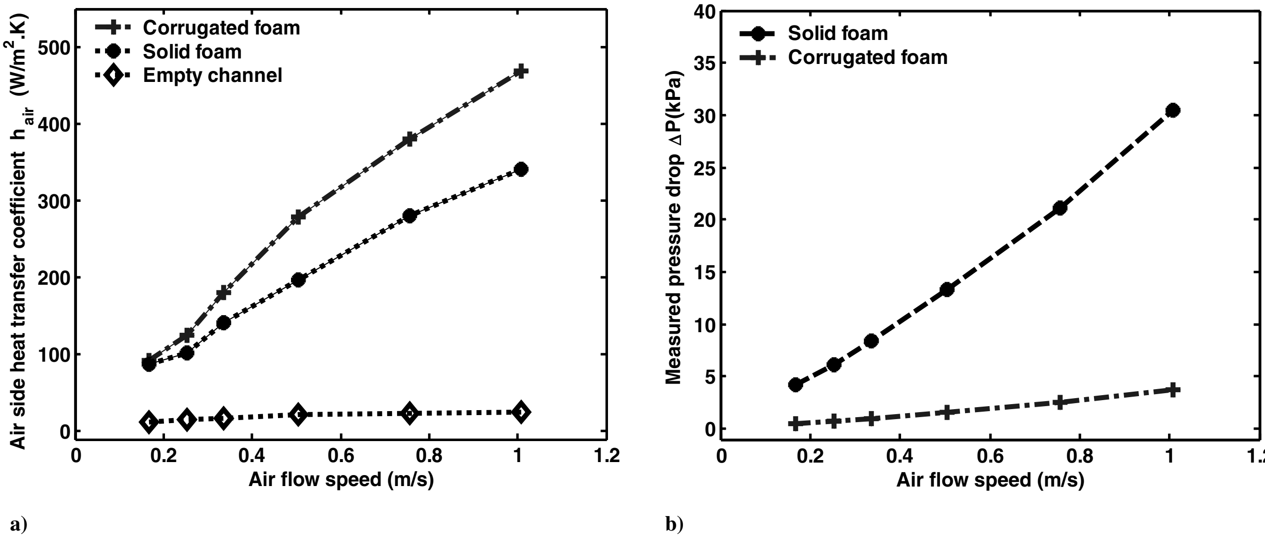

Fig. 5 Results of a) air-side heat transfer coefficient h_{air} and b) solid and corrugated foam Δp (empty channel is negligible).

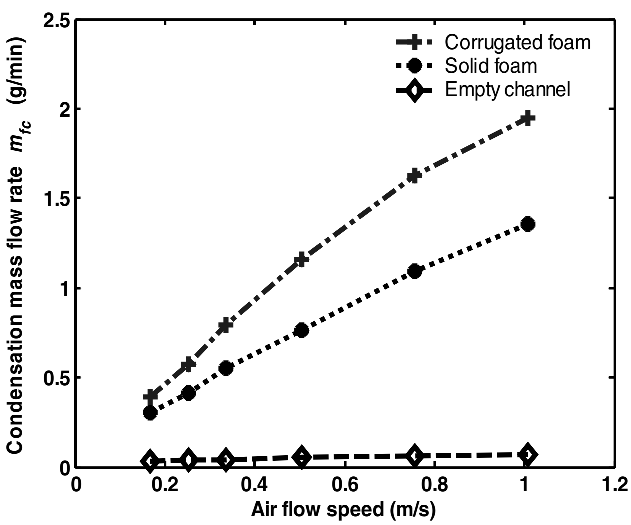

Fig. 6 Room-temperature condensation rate.

Although the presence of the solid carbon foam results in a substantial increase in the air-side heat transfer coefficient, the pressure drop across the foam is 30.8 kPa. The pressure drop for the corrugated foam was 3.5 kPa at an airflow velocity of 1 m/s, a reduction by a factor of 8.8 when compared with the solid foam. This is significant evidence that corrugated carbon foam has a much lower pressure drop than solid carbon foam. Corrugation shortens the airflow length through the foam. The air speed within the corrugated foam is also lower than that in the solid foam. Because the pressure drop across foams is directly proportional to the flow length and velocity, corrugation significantly reduces pressure drop.

Figure 6 shows the room-temperature ($22 \pm 0.5\,^\circ$C) condensation rate for the empty channel, solid carbon foam, and corrugated carbon foam. The condensation rate at $V = 1$ m/s for the corrugated and solid carbon foams are and 2 and 1.4 g/ min, respectively.

The condenser with the corrugated carbon foam exhibited an 18-fold increase in heat transfer coefficient (25.9 and 469 $\mathrm{W/m^2 \cdot K}$ at 1 m/s for this 5-cm-long carbon foam). The higher heat transfer coefficients lead to a significant reduction in base heat transfer area needed for a similar heat transfer/condensation rate.

V. Conclusions

The development of an effective cold head for liquefaction of gaseous hydrogen and its subsequent densification to subcooled liquid hydrogen requires a high-efficiency condenser. A novel concept for a heat sink using carbon foam blocks was proposed. The cold head using carbon foam for liquefaction of cryogens was designed and tested, showing that this is a viable technology, worthy of further study. High-thermal-conductivity carbon foam was used to increase the heat transfer coefficient. These experiments used air and vapor/liquid FC-87 to simulate helium and gaseous/liquid hydrogen. Corrugated foam was used as an alternative flow design, resulting in a significant reduction in the flow resistance. These results show that this flow arrangement can significantly reduce the pressure drop and heat transfer performance is improved. Experimental results with air and vapor/liquid FC-87 show that carbon foam-based heat sinks can provide a heat transfer coefficient that is 18 times greater than those of conventional air-channel heat sinks at low speed (1 m/s).

Acknowledgments

The authors gratefully acknowledge the financial support of NASA John H. Glenn Research Center at Lewis Field, NASA Kennedy Space Center, and Florida Space Grant Consortium.

References

[1] Notardonato, W., "Analysis and Testing of an Integrated Refrigeration and Storage System for Liquid Hydrogen Zero Boil-Off, Liquefaction, and Densification," Ph.D. Dissertation, Dept. of Mechanical and Aerospace Engineering, Univ. of Florida, Gainesville, FL, Aug. 2006.

[2] Zhou, L., Kapat, J., Chow, L., and Lei, S., "Design of a High Performance Cryocooler for Propellant Liquefaction and Storage on Mars," *Proceedings of the ASME Heat Transfer Division*, Vol. 2, American Society of Mechanical Engineers, New York, 5–10 Nov. 2000, pp. 331–338.

[3] Webb, R. L., *Principles of Enhanced Heat Transfer*, Wiley, New York, 1994.

[4] Calmidi, V. V., and Mahajan, R. L., "Forced Convection in High Porosity Metal Foams," *Journal of Heat Transfer*, Vol. 122, No. 3, 2000, pp. 557–565.
doi:10.1115/1.1287793

[5] Leong, K. C., and Jin, L. W., "Effect of Oscillatory Frequency on Heat Transfer in Metal Foam Heat Sinks of Various Pore Densities," *International Journal of Heat and Mass Transfer*, Vol. 49, Nos. 3–42006, pp. 671–681.
doi:10.1016/j.ijheatmasstransfer.2005.08.015

[6] Gallego, N. C., and Klett, J. W., "Carbon Foams for Thermal Management," *Carbon*, Vol. 41, No. 7, 2003, pp. 1461–1466.
doi:10.1016/S0008-6223(03)00091-5

[7] Klett, J. W., Tee, C. C., Stinton, D. P., and Yu, N. A., "Heat Exchangers Based on High Thermal Conductivity Graphite Foam," *Proceedings of the 1st World Conference on Carbon*, Eurocarbon, Berlin, 2000, pp. 244–245.

[8] *CN8590 Series 1/32 DIN Temperature/Process Controllers: User's Guide* [online manual], OMEGA Engineering, Stamford, CT, 1999, www.omega.com/Manuals/manualpdf/M2386.pdf [retrieved Oct. 2008].